Available online at www.sciencedirect.com
ScienceDirect
Journal of the European Ceramic Society 29 (2009) 1657–1664
www.elsevier.com/locate/jeurceramsoc

Mechanical properties of NiO/Ni–YSZ composites depending on temperature, porosity and redox cycling

Mikko Pihlatie [a,b,*], Andreas Kaiser [a], Mogens Mogensen [a]

[a] *Risoe National Laboratory for Sustainable Energy, Technical University of Denmark, POB 49, DK-4000 Roskilde, Denmark*
[b] *Helsinki University of Technology, Department of Engineering Physics, POB 4100, FI-02015 TKK, Finland*

Received 20 August 2008; received in revised form 27 October 2008; accepted 29 October 2008
Available online 20 December 2008

Abstract

The Impulse Excitation Technique (IET) was used to determine the elastic modulus and specific damping of different Ni/NiO–YSZ composites suitable for use in solid oxide fuel cells (SOFC). The porosity of the as-sintered samples varied from 9 to 38% and that of the reduced ones from 31 to 52%. For all samples a linear relation between Young's modulus and porosity was found. The temperature dependency of the mechanical properties of both as-sintered and reduced composites was investigated by IET up to 1200 °C. In the as-sintered state, first an increase and peak of stiffness coinciding with the Néel temperature, 250 °C, of NiO was observed. Above this temperature, a linear decrease occurred. Specific damping showed a peak at 170–180 °C and increased above ca. 1000 °C in NiO–YSZ. In the reduced state the elastic modulus decreased linearly with temperature; specific damping increased above ca. 600 °C and was found to be very dependent on microstructure. Damage caused by redox cycling degraded the elastic properties of the composites. Degradation started linearly from 0.5 to 0.6% redox strain leading to macroscopic sample failures at about 2.5% dL/L_o. A simple continuum elastic damage model was fitted to the degradation data.

Keywords: Fuel cells; Mechanical properties; Composites; Plasticity; SOFC

1. Introduction

Solid Oxide Fuel Cells (SOFC) continue to be a promising energy conversion technology for an environmentally benign power generation capable of utilising different hydrocarbons as well as hydrogen as the fuel. Despite active search for alternatives, Ni–YSZ composites are widely used as anode side components. In a popular flat SOFC design such cermets serve as structural materials for the electrochemical devices.[1] Requirements for Ni–YSZ anode supports are sufficient mechanical stability as well as strength, stiffness, porosity, and electrical conductivity. An additional challenge for the Ni-based SOFC is the situation where an operating cell is re-oxidised from the anode side and chemically induced strains from the Ni oxidation expand the whole structure, resulting in the so called redox instability problem for SOFC.[2] If the nickel is oxidised to NiO, the related volumetric expansion exerts large stresses on both the anode composite internally, and through bulk expansion of the anode support, on the cell as a whole.[3–5]

The mechanical properties of the anode supported SOFC are dominated by the thick (300 μm or above) anode support, and therefore knowledge of its mechanical behaviour is of importance for cell design and modelling. Giraud and Canel have studied elastic properties of YSZ, Ni–YSZ and LSM up to high temperature.[6] Radovic and Lara-Curzio examined the elastic properties of Ni-based anode composites as a function of porosity of up to 25% (roughly 25–41% in the reduced state), and as a function of the degree of NiO reduced. They found that the stiffness, fracture toughness and strength of the composites decreased with porosity, although upon reduction of the NiO to Ni the fracture toughness and strength increased due to the presence of the ductile Ni phase.[7,8] Morales-Rodriques et al. have conducted experiments on creep behaviour of Ni–YSZ composites at high temperature and different oxidation states and showed that the ceramic component largely controls the creep behaviour; reduction of NiO to nickel generally lowers

* Corresponding author. Present address: VTT Technical Research Centre of Finland, P.O. Box 1000, FI-02044 VTT, Finland.
Tel.: +358 45 1103464/400 430395.
E-mail addresses: mikko.pihlatie@iki.fi, mikko.pihlatie@vtt.fi (M. Pihlatie).

0955-2219/$ – see front matter © 2008 Elsevier Ltd. All rights reserved.
doi:10.1016/j.jeurceramsoc.2008.10.017

the creep resistance due to the metallic phase.[9,10] Selcuk and Atkinson have reported the mechanical behaviour of materials relevant for SOFC electrolytes presenting an overview of different available correlations for elastic properties vs. porosity.[11,12] Further, Radovic et al. compared different techniques available for characterisation of mechanical properties for ceramic composites and two techniques, namely Resonant Ultrasound Spectroscopy (RUS) and Impulse Excitation Technique (IET) were found preferable.[13] In the work of Roebben et al., IET was applied in the characterisation of the elastic properties and damping of yttria stabilised zirconia polycrystals (Y–TZP) up to high temperatures, yttria content being 2–3 mol%.[14,15] At elevated temperatures the analysis showed an internal friction peak due to elastic dipole ($Y'_{Zr}V''_{O}$) relaxation at 490 K and low temperature degradation (LTD) due to tetragonal–monoclinic phase transformation at around 500 K where the thermodynamic driving force for the transformation is largest. Whether or not the LTD was observed depended on the yttria content (partial stabilisation), microstructure (homogeneity of Y-doping) and the temperature history.[14,15] Regarding redox stability of Ni–YSZ composites, the IET has also been applied to assess changes in mechanical properties due to redox cycling; after two redox cycles carried out at 800 °C with permanent elongation of about 0.5% dL/L_o no change in the elastic properties was found.[16]

This paper discusses determination of mechanical properties, using IET, of different NiO–YSZ and Ni–YSZ composites as a function of temperature up to 1200 °C. Several different batches of composites were prepared by ceramic processing and tested. Mechanical degradation of the composites due to internal damage from redox cycling was investigated in an attempt to connect the dimensional behaviour of such structures with gradually deteriorating mechanical properties, finally leading to a loss of integrity of the composite.

2. Experimental

2.1. Ceramic processing and the samples

The samples tested were manufactured from commercial NiO and 3YSZ powders using standard ceramic processing techniques. The powders were ball milled in ethanol-based slurries using dispersants and organic binders. The porosity range 10–38% after sintering was achieved by variation of the solids composition as well as the particle size distributions of the powders used. The slurries were tape cast and cut to green plates, which after sintering at 1300–1400 °C yielded ceramic plates of 0.3–0.7 mm thickness and 70–80 × 20–25 mm^2 size. Some of the samples tested are similar to those tested in.[17] Some rectangular thin plates were also laser cut directly from as-sintered larger anode supports or half cells into a size of 20 × 75 mm^2. The thinnest plates had some tendency to warp upon redox cycling, which is a sign of either non-uniform oxidation or slightly anisotropic material e.g. in terms of surface condition on both sides of the plate. The structural stiffness arising from the warping of the samples alters the resonant vibration spectrum. In order to overcome this, some samples were prepared by laminating 2–3 green tapes to obtain approximately 1 mm thick samples. After this, up to 8 redox cycles could be measured.

The solids composition of the samples was 50–55 wt-% NiO and 45–50 wt-% YSZ. The theoretical density (TD) was calculated from the composition to be between 6.34 and 6.40 g/cm^3. The total porosity of the samples could be calculated geometrically and varied from 9 to 38% in the as-sintered state. In the reduced state the tested samples had total porosities ranging from 31 to 52%. The data measured at room temperature arise from a total of 19 different green tapes in the as-sintered state and 16 different tapes in the reduced state.

2.2. Testing equipment

The mechanical tests were carried out using IET equipment from IMCE NV, Genk, Belgium.[18] Impulse excitation offers fast and repeatable measurements of thin plates with a well-defined geometry. For room temperature measurements, the resonant frequency and damping analyser RFDA System 23 was used. The method is based on detecting characteristic vibration frequencies of samples supported at the nodal points by thin wires. The resonant flexural frequencies of vibration are deduced from the digital signal by Fast Fourier Transform (FFT).

The Young's and shear moduli are calculated for well-defined isotropic and homogeneous materials of different geometries using ASTM E 1876-99 and ASTM C 1259 standards. When the fundamental resonant frequency as well as the mass and the dimensions of the sample are accurately known, the Young's modulus is calculated as[19]

$$E = 0.9465\frac{mf_f^2}{b}\frac{l^3}{d^3}T_1 \quad (1)$$

where m is sample mass, f_f is the fundamental resonant frequency, b, l and d the width, length and thickness of the bar respectively, and T_1 a correction factor depending on the thickness-to-length ratio and Poisson ratio of the material. For the samples considered here the thickness-to-length ratio is small (0.005–0.008) and the value of T_1 very close to unity.

Reproducibility of the measurements was good. The main source of uncertainty comes from sample thickness. The calculated moduli are cubically dependent on the length and inverse cubically dependent on the thickness of the sample as shown in (1); the standard deviation in thickness of the sample population based on three measurements per sample varied from 0.3 to 3.7% with the mean at 1.3%. The standard deviation in length was 0.2% (based on three length measurements per sample). The flexural vibration mode was used for all samples; additionally the torsional mode yielding the shear modulus was applied for two samples. At room temperature, a microphone was used to detect the vibrations. The high temperature measurements were carried out at IMCE NV in Belgium, using the RFDA combined with the HTVP 1600 furnace and a laser vibrometer in either air (oxidised samples) or 5% H_2 diluted with N_2 (reduced samples). The heating rate used in the high-temperature tests was 3–4 °C/min while the cooling rate was 1.8–2.8 °C/min. For the

room temperature measurements, the sample treatments were done in a separate furnace.

2.3. Reduction–oxidation tests

In order to examine whether the initial reduction temperature and related microstructural differences reflect in the mechanical properties of the bulk, NiO–YSZ plates were reduced at three different temperatures of 600, 850 and 1000 °C. The elastic moduli of the samples were measured by IET both before and after reduction. Further steps of complete oxidations and reductions were carried out for several samples at temperatures between 750 and 850 °C. The procedure used in the reduction/oxidation of the samples was to first heat up in an atmosphere similar to the previous treatment and stabilise for at least an hour. The reduction/oxidation step was always carried out in isothermal conditions. As a part of gas changes oxidising/reducing, a short flush of N_2 was always implemented in between. The reducing gas used was 9% H_2 in N_2. During the furnace anneals, the samples were either loosely sandwiched between ceramic plates or placed free-standing on top of a plate. After each step, the porosity of the sample was estimated from the sample dimensions determined using digital Mitutoyo callipers, and weight by Mettler Toledo gauges. The Cumulative Redox Strain (CRS)[17] was used for the sample length change dL during redox cycling, relative to the initial as-sintered cold length L_o. Eight redox cycles were carried out for two laminated samples, the first five at 750 °C and the last three at 790 °C. During the first three redox cycles both the oxidised and reduced condition were measured.

2.4. On the theory of viscoelasticity

In an elastic material, stress and strain are linearly dependent on each other through Young's modulus. When the stress–strain relationship additionally depends on time the material is called viscoelastic. For example, a step change in stress results in a delayed strain response. For dynamic considerations in a free or forced vibration the Young's modulus can be replaced by the dynamic or complex modulus,

$$E^* = E' + iE'' \tag{2}$$

In this complex notation E' is the elastic (storage) modulus and E'' the plastic (loss) modulus. The time lag between stress and strain, caused by damping or internal friction within the material, is the loss angle ϕ by which the plastic (loss) modulus is lagging the elastic (storage) modulus, $\tan\phi = E''/E'$.

In the present automatic analysis the specific damping due internal friction is fitted using a linear combination of exponentially decaying sinusoidal functions with amplitude A [of the form $A(t) = A_o \exp(-kt)\cdot\sin(\omega t + \phi)$] where the signal stems from a mechanically excited sample in free flexural vibration. When the loss tangent is small ($\tan\phi < 0.1$), the following holds for the specific damping Q^{-1} of the material with good accuracy[18,20]:

$$Q^{-1} = \tan\phi = \phi = \frac{k\pi}{f_r}, \tag{3}$$

where k is the fitted parameter in the exponential decay function and f_r the respective resonant frequency. In some literature the specific damping Q^{-1} is also called the damping ratio. In many materials, viscoelasticity and damping are governed by thermally activated processes and further are dependent on the frequency f of the applied stress according to

$$\tan\phi = g(f)\exp\left(-\frac{E_a}{RT}\right), \tag{4}$$

E_a being an activation energy, R the gas constant and T the absolute temperature. When a material is at a high homologous temperature, that is, the absolute temperature exceeds a fraction of about 0.3–0.5 of the melting temperature, viscoelastic effects like damping and creep manifest themselves. The dominating mechanism through which mechanical energy is dissipated in a material depends on the frequency at which an oscillation takes place. For example, low frequency relaxation processes include diffusional creep and grain boundary slip, whereas larger relative contributions at higher frequencies arise from e.g. point defect, elastic dipole or thermoelastic relaxation.[21] Composite materials have additional effects where the different phases give partial contributions to the bulk properties. Also, porosity can constitute a third phase having zero viscoelastic properties. The properties of the composite depend on the composition (volume fractions), shape and microstructure of the phases and/or inclusions and the nature of the interfaces. In a ceramic–metal Ni–YSZ composite at elevated temperatures, the metal component is expected to show higher plasticity due to its higher homologous temperature. How the composite behaves in viscoelastic terms as a whole depends on the microstructure; particle size distributions, interfacial condition and interface length as well as mechanical interaction between the phases. Changes in the microstructure are expected to reflect themselves in damping behaviour.

2.5. Correlating Young's modulus and porosity

The elastic properties used for tetragonal zirconia polycrystals (TZP), NiO and Ni were taken from the literature and are shown in Table 1. As the solids composition of the composite is usually known, the moduli of a fully dense composite can be estimated e.g. by using the linear rule of mixtures and volume fractions of the constituents. In practice, the Young's moduli of TZP, NiO and Ni are relatively close to each other, so the effect from compositional change is not very large. For the dependency of elastic properties on porosity, different correla-

Table 1
Elastic properties of TZP, NiO and Ni in the literature.[11,8,22] E is Young's modulus, G is shear modulus and ν the Poisson ratio.

	E (GPa)	G (GPa)	ν Poisson ratio
TZP	213–218[a]	81	0.33
	216[b]		
NiO	220	84	0.3
Ni	200	77	0.3

[a] Estimate at full density using correlations[11].
[b] Single crystal data[11].

Table 2
Linear, exponential and non-linear correlations for Young's modulus vs. porosity available in the literature for NiO–YSZ composites.[11].

	Correlation for E	Parameter b	E_o
Linear	$E = E_o(1 - bp)$	2.10	205.46
Exponential	$E = E_o \exp(-bp)$	2.48	207.13
Non-linear	$E = E_o\left[1 - \frac{bp}{1+(b-1)p}\right]$	2.55	207.22

Table 3
Parameters from least squares linear fitting of the measured Young's modulus vs. porosity p. The goodness of fit is given by the R^2 value ($R^2 = 1$ indicating a perfect fit).

	$E = E_o(1 - bp)$	E_o (GPa)	b	R^2
Oxidised		206.88	2.118	0.986
Reduced		205.93	1.756	0.954

tions have been reported in the literature. Atkinson and Selcuk have studied this also referring work from different authors, giving three correlations for the oxidised NiO–YSZ composite.[11] These linear, exponential and non-linear correlations are summarised in Table 2. Additionally, a more theoretical model based on composite spheres has been discussed in the literature.[8,11] The dependency of the elastic properties on temperature has been less reported in the literature. Young's modulus is known to decrease with temperature for most materials, typically in a linear manner.

3. Results and discussion

3.1. Young's modulus vs. porosity

The Young's moduli measured at room temperature for totally 97 as-sintered samples are shown in Fig. 1. The results exhibit a largely linear dependency on porosity. A few half cells were measured and they agree with the NiO–YSZ composite data. Comparison with the three correlations given in Table 2 shows that the linear correlation produces the best agreement with the measured data. The parameters of a linear least squares fit to the data in Fig. 1 are shown in Table 3. The best fit to the present data agrees well with the linear correlation reported for similar NiO–YSZ composites in.[11] The non-linear and exponential correlations taken from the literature, Table 2, lose their accuracy in predicting the present data when total porosity (as-sintered) exceeds about 20%. In other words, the non-linear and exponential correlations tested behave more or less linearly up to porosities of about 20%.

The results on reduced Ni–YSZ cermets measured at room temperature comprise 54 samples and are shown in Fig. 2. The samples were reduced at temperatures between 600 and 1000 °C; no difference in the Young's modulus depending on the initial reduction temperature could be observed. The porosity of the samples is higher than in the as-sintered state due to the smaller molar volume of Ni as compared to NiO. A linear correlation was considered sufficient to fit the data in a satisfactory way. The obtained Young's modulus vs. porosity by a free linear least squares fit to the data is shown in Fig. 2, with the parameters presented in Table 3. Fig. 2 contains also reduced half cells as well as four measurement points where the samples have been partially re-oxidised to Degree of Oxidation (DoO) of 0.23, 0.30, 0.53 and 0.61, respectively. When Young's moduli of the partially oxidised samples are plotted in Fig. 2, after calculation of the TD and porosity, the elastic properties follow the correlation for reduced samples quite well.

One as-sintered and one reduced sample were measured in the torsional vibration mode to determine the Shear modulus of the composites. The measured Young's and shear moduli of these samples as well as the calculated Poisson's ratio are presented in Table 4. The obtained values for the Poisson's ratio are slightly higher than those reported in the literature for TZP, NiO and Ni (Table 1).

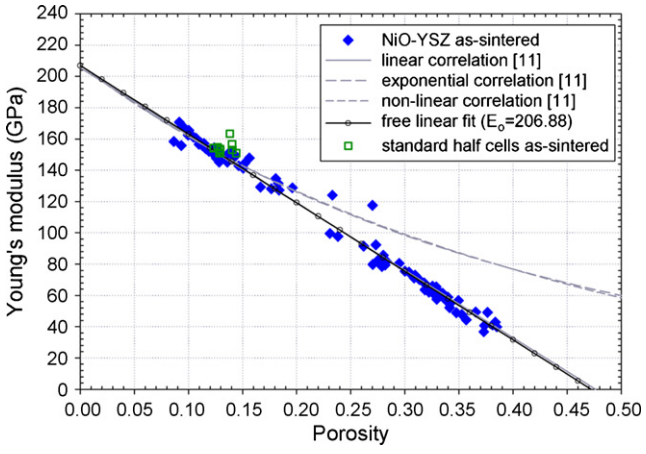

Fig. 1. Young's modulus of as-sintered NiO–YSZ composites as a function of total porosity with a linear correlation fitted to the data (the black line) and other correlations reported in the literature (the gray lines). Half cell data are consistent with NiO–YSZ composites.

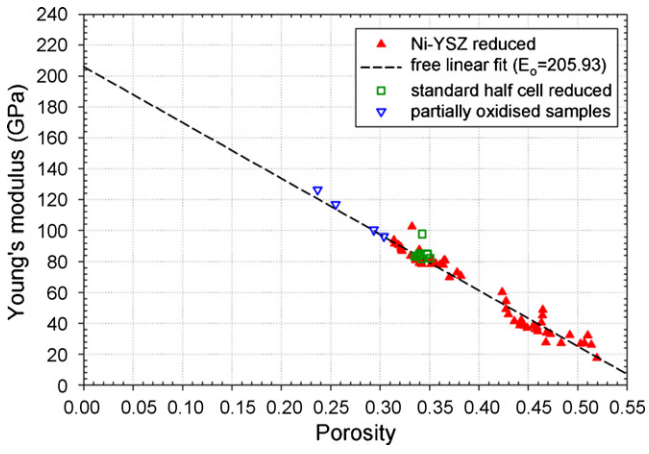

Fig. 2. Young's modulus of reduced Ni–YSZ composites as a function of total porosity including a linear correlation fitted to the data. Half cell data in the reduced state are consistent with the Ni–YSZ cermets. The graph shows also the Young's modulus of four partially oxidised samples.

Table 4
Measured Young's and shear moduli as well as the calculated Poisson ratio for as-sintered and reduced NiO/Ni–YSZ composites.

	Young's modulus (GPa)	Shear modulus (GPa)	Poisson's ratio
As-sintered NiO–YSZ	127.3	49.7	0.391
Reduced Ni–YSZ	80.9	31.4	0.387

3.2. Young's modulus vs. temperature

3.2.1. NiO–YSZ

Results from a high temperature flexural mode test of an as-sintered sample up to 1200 °C are shown in Fig. 3. The initial room temperature value of the Young's modulus will depend on the porosity of the sample as shown in Fig. 1. During the high-temperature test in Fig. 3, the Young's modulus was relatively constant from room temperature to about 180 °C, after which the modulus increased by about 6% and peaks at about 250 °C. After reaching the peak, a more or less linear decrease in the modulus could be observed up to about 1100 °C, after which the modulus departed slightly downwards from the linear trend. Relatively good reproducibility was obtained during cool-down. For the specific damping, a peak reaching up to 0.01 on heating and 0.008 on cooling down was measured at about 160–180 °C. Above about 250 °C the damping returned to below 0.005. On heating, the specific damping started slowly increasing above about 950 °C and reached about 0.03 at 1200 °C.

The damping behaviour of partially stabilised TZP (2–3% YSZ) have been studied by Roebben et al.[15], who saw a damping peak to due relaxation of the elastic dipoles ($Y'_{Zr}V''_{O}$) at 217 °C. The damping peak measured here occurs consistently at a somewhat lower temperature. No further investigations were carried out in order to confirm whether the reversible low temperature damping was in this case related to the elastic dipole relaxation. The change in elastic properties between 200 and 260 °C and the peaking of the Young's modulus at about 250 °C coincides with the transition of NiO from antiferromagnetic to paramagnetic at the Néel temperature of 250 °C. Earlier, du Plessis et al. have reported the elastic properties of NiO single crystals using an ultrasonic technique. They found an anomalous jump in the elastic modulus at the Néel temperature, possibly due to second order phase transition.[23] The elastic transient observed at about 250 °C is thus probably due to the elastic anomaly in NiO at that temperature. The coefficient of thermal expansion (CTE) was studied in dilatometry and the measurement shows a peak at about 250 °C, in agreement with what was also reported by e.g. Mori et al.[24].

3.2.2. Ni–YSZ

Fig. 4 shows the measured Young's modulus as a function of temperature for a Ni–YSZ cermet pre-reduced at 1000 °C. The measured total porosity of the sample was 38% and the measured elastic modulus at room temperature was 72.9 GPa. The Young's modulus decreases more or less linearly with temperature down to 51.8 GPa at 1000 °C. A peak in damping at 160–180 °C similar to that in Fig. 3 was observed; this confirms that it should arise from the TZP phase. After the low temperature damping peak, the damping decreases although less than in the as-sintered sample. Increased specific damping is observed when the temperature exceeds about 600 °C; the damping measured at the ramp terminal temperature 1000 °C was about 0.025. The increase in damping occurring at a lower temperature in the reduced sample as compared to the oxidised state can be ascribed to the metallic nickel component having a much lower melting temperature than the ceramic NiO (T_M = 1450 and 1960 °C of Ni and NiO, respectively).

The dependence of specific damping on micro structural features was examined by conducting another experiment for a

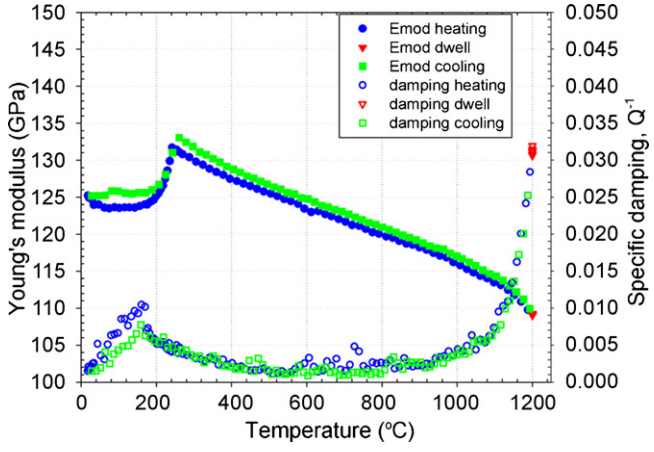

Fig. 3. Young's modulus and specific damping as a function of temperature during heat-up and cool-down of an as-sintered NiO–YSZ composite. Young's modulus peaks at around 250 °C decreases linearly at temperatures above that. For specific damping, a small peak at 160–180 °C as well as an increase above 1000 °C is observed.

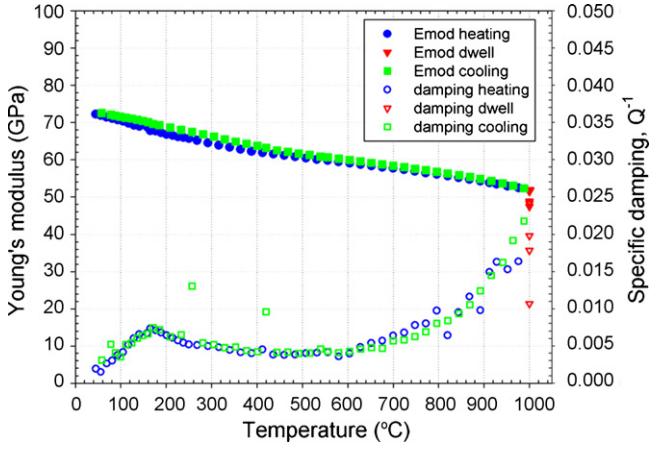

Fig. 4. Young's modulus and specific damping as a function of temperature during heat-up and cool-down of a Ni–YSZ composite sample pre-reduced at 1000 °C and tested under reducing atmosphere. Elastic modulus decreases linearly with temperature. Specific damping shows a peak at 160–180 °C and increases above 600 °C.

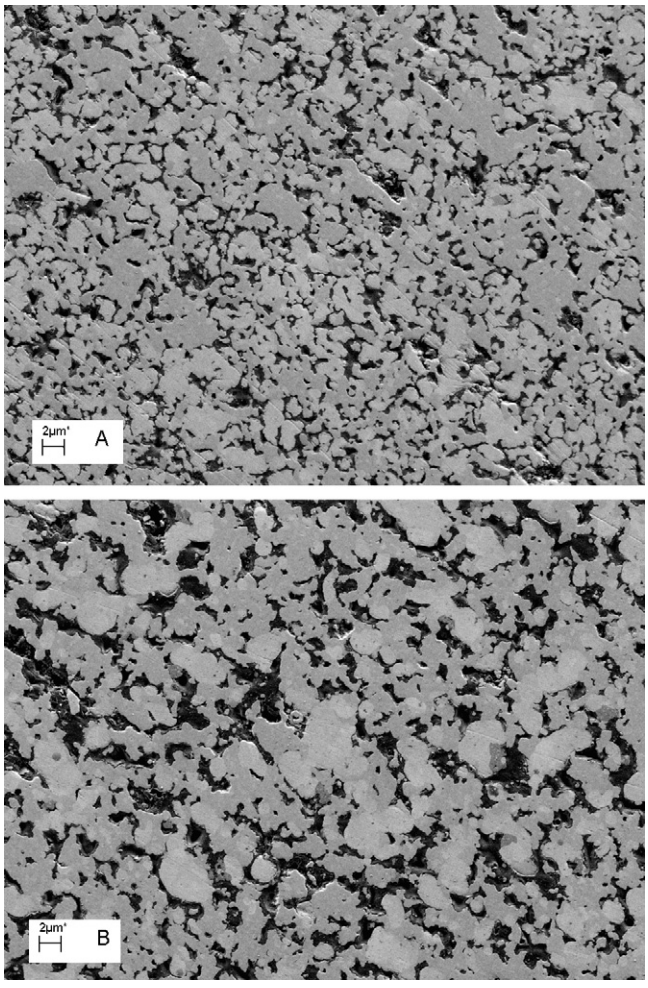

Fig. 5. Secondary electron image using a FE SEM and the low voltage charge contrast technique on a polished cross-section of a Ni–YSZ composite reduced 96 h at 600 °C (A) and 1000 °C (B), showing growth in Ni grains due to sintering. The lighter gray is Ni, darker gray YSZ and black areas porosity.

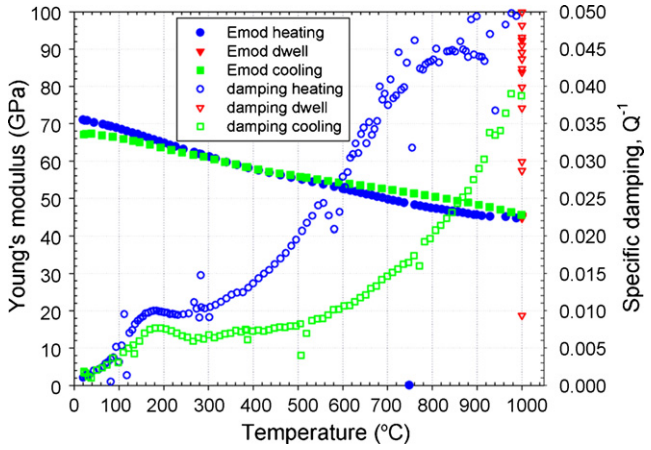

Fig. 6. Young's modulus and specific damping as a function of temperature during heat-up and cool-down of a Ni–YSZ composite sample pre-reduced at 600 °C and tested under reducing atmosphere. Damping is shown to be a sensitive function of the microstructure with higher damping related to finer microstructure. A decrease in damping due to Ni sintering is observed during and after high temperature operation.

sample pre-reduced at 600 °C. The lower reduction temperature results in a finer microstructure, because the metallic nickel particles undergo less sintering during the reduction treatment.[25,26] This is evident looking at Fig. 5A (sample reduced at 600 °C) and 5b (sample reduced at 1000 °C), where lighter gray is metallic nickel, darker gray YSZ and black areas porosity. The images were taken using a Zeiss Supra FEG SEM and the low voltage charge contrast technique.[27] The elastic modulus and specific damping are shown in Fig. 6. The measured elastic modulus is essentially the same as after high temperature reduction shown in Fig. 4. The damping peak at 160–180 °C can be observed as previously. During the heat-up, measured damping is clearly higher reaching about 0.05 at 1000 °C. During the 1 h hold at 1000 °C, damping decreased from 0.05 to roughly 0.04, and during cool-down showed lower values than during heat-up.

The reduced Ni–YSZ cermets show viscous activation generally at a lower temperature than the oxidised ones, and additionally a more complex behaviour above the low temperature-damping peak. The sample reduced at 600 °C shows highest specific damping, furthermore the damping remains high when elevating the temperature further (no decrease in damping after the 170 °C peak) and starts increasing further when exceeding about 300 °C. When cooling the same sample down from 1000 °C, damping is clearly less as observed in Fig. 6. The specific damping is larger in fine microstructure and well connected interfaces, which is the case initially for the sample pre-reduced at 600 °C. The decrease arises from microstructural changes and loss of ceramic–metal interface due to sintering of Ni at high temperatures. The sample reduced at 1000 °C showed the lowest and the most stable damping of the cermets. In this case the microstructure and degree of Ni sintering originated from the pre-reduction and remained largely unaltered during the mechanical test.

3.3. Effects from redox cycling

Results for Young's modulus, CRS and specific damping are shown in Figs. 7 and 8. The two samples show initially about 130–140 GPa elastic modulus and 80 GPa after the initial reduction; this decrease is largely due to porosity change. Upon cyclic re-oxidations, the CRS increases gradually reaching 2–2.5% after the 6th or 7th re-oxidation. The Young's modulus of the samples decreases quite linearly with the CRS as can be observed in Fig. 9. The relatively linear degradation in the elastic properties starts at about 0.5% dL/L_o and in the measured series proceeded all the way down to 80% loss (data up to 70% shown in the figure). Gradually increasing macroscopic damage could be visually observed in the sample starting from about 1% CRS. Integrity of the samples was lost due to macroscopic fragmentation at around 2.5% CRS and measured Young's modulus below ca. 30 GPa.

The stiffness of a sample is an integral measure of the mechanical properties representing the bulk material. We regard the Ni–YSZ cermet as a porous composite where the YSZ constitutes a rigid ceramic backbone and the Ni a second percolating phase. Upon re-oxidation of the Ni the expansion can exert large local stresses on the ceramic structure and create damage, as dis-

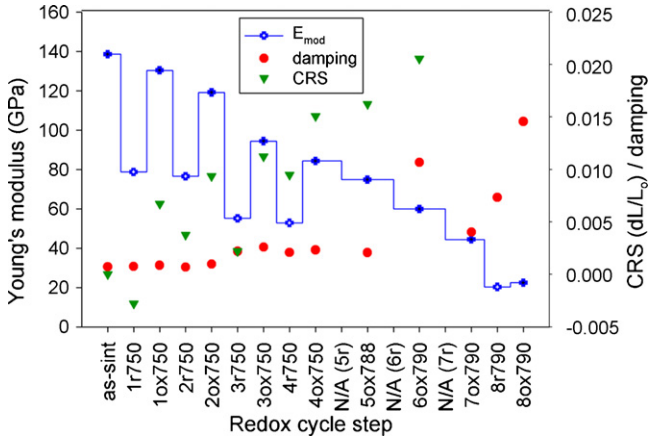

Fig. 7. Elastic properties and damping of Ni–YSZ composite (sample 1) as a function of reduction-oxidation steps carried out isothermally at 750–790 °C. Elastic modulus shows stepwise decrease while the Cumulative Redox Strain (CRS) and damping are increasing with the number of redox cycles. The abscissa point acronyms stand for cycling step number, *r* = reduced/ox = oxidised state, and a number indicating temperature, e.g. '2ox750' means the 2nd re-oxidation of the sample carried out at 750 °C. The data on the 5th, 6th and 7th reduction are missing (N/A).

cussed e.g. by Klemensø and Mogensen.[28] This internal damage is first microscopic and becomes macroscopic through crack propagation. The porous composite can be viewed as a complex three-dimensional structure composed of a large number of Hookean springs or anelastic spring-dashpot elements connected in series and in parallel. The bulk stiffness of a sample arises from the integral effect of these elastic elements. We propose that when microscopic or macroscopic damage is created in the structure, in this case by redox cycling, it is equal to removing elastic elements from the bulk structure. Therefore, a decrease in the measured Young's modulus is observed. In macroscopic terms the Cumulative Redox Strain is a measure

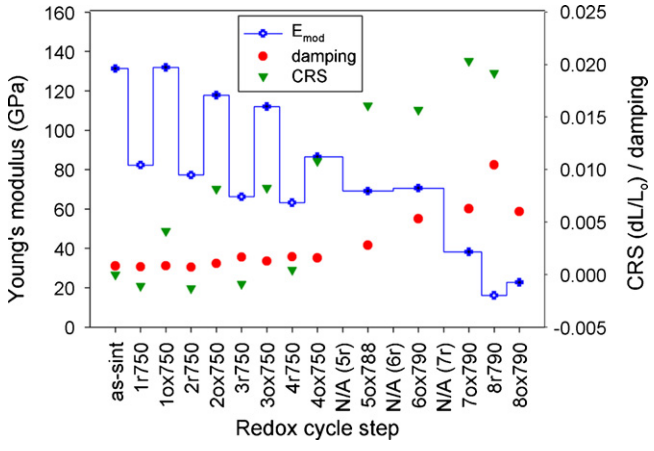

Fig. 8. Elastic properties and damping of Ni–YSZ composite (sample 2) as a function of reduction–oxidation steps carried out isothermally at 750–790 °C. Elastic modulus shows stepwise decrease while the Cumulative Redox Strain (CRS) and damping are increasing with the number of redox cycles. The abscissa point acronyms stand for cycling step number, *r* = reduced/ox = oxidised state, and a number indicating temperature, e.g. '2ox750' means the 2nd re-oxidation of the sample carried out at 750 °C. The data on the 5th, 6th and 7th reduction are missing (N/A).

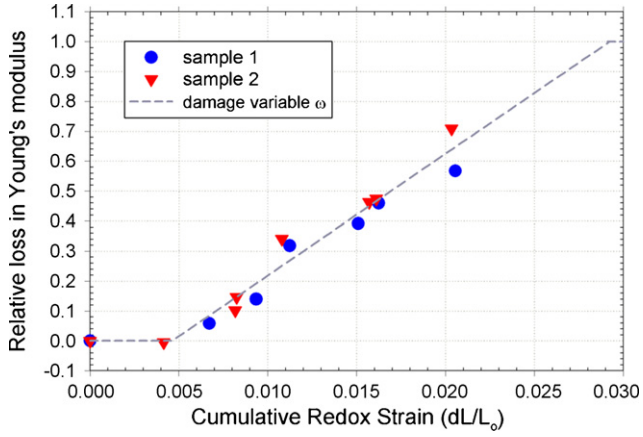

Fig. 9. Mechanical degradation in terms of relative loss of elastic modulus of NiO–YSZ composites in the oxidised state during redox cycling, as a function of CRS the cumulative sample length change caused by the redox cycling. Largely linear elastic degradation is observed with CRS. A damage variable ω depending on CRS was fitted to the measured data.

of the irreversible dimensional change in the composite due to redox cycling. Our results suggest that the CRS is more or less linearly related to the microscopic and macroscopic damage taking place in the composite and manifesting itself as loss of stiffness. An isotropic continuum damage model for elastic degradation can be expressed in a simple form as

$$E = (1 - \omega)E_o \tag{5}$$

where E is the elastic modulus, ω the damage variable having values from 0 to 1, and the initial modulus is E_o. Fitting a parameter ω (CRS) to the present redox degradation data yields the damage variable shown in (6) and also depicted graphically in Fig. 9. As a measure of the quality of fit, the R^2 value of the fit was 0.949.

$$\omega(CRS) = \begin{cases} 0, & CRS < 0.0046 \\ 40.655 \cdot CRS - 0.1879, & 0.0046 \le CRS < 0.0292 \\ 1, & CRS \ge 0.0292 \end{cases} \tag{6}$$

4. Conclusions

Composites of Ni–YSZ and NiO–YSZ were tested for elastic properties at room temperature and viscoelastic properties elevated temperatures. The Impulse Excitation Technique was used for the measurements.

Total porosities of the samples were determined geometrically. The measured Young's moduli of the composites show a linear dependence on porosity. Linear correlations were fitted to the elastic property data with porosities in the oxidised state ranging from 9 to 38% and in the reduced state from 31 to 52%.

The dependence of the Young's modulus and specific damping as a function of temperature was determined both in the oxidised and reduced state. In the oxidised state, we found a reversible steep increase in Young's modulus taking place between about 200 and 260 °C, with a peak at 250 °C. The tem-

perature of this transient coincides with the Néel temperature of NiO. Above 260 °C a largely linear decrease of Young's modulus with temperature was measured up to 1200 °C.

The elastic properties in the reduced state were measured for samples pre-reduced at a low (600 °C) and a high (1000 °C) temperature. The Ni–YSZ composite shows linear decrease in the Young's modulus with temperature up to 1000 °C and little effect from the initial reduction temperature.

Specific damping of the composite determined from the fundamental flexural resonant frequency showed only minor, if any, differences between samples with different treatments when measured at room temperature. High temperature tests showed (i) a damping peak at 160–180 °C; (ii) increase in damping of the NiO–YSZ composite above roughly 1000 °C; (iii) increase in damping starting at lower temperatures in the reduced cermets as compared with the oxidised state; and (iv) the dependence of the damping in the Ni–YSZ composite on microstructure, where fine microstructure after low temperature reduction results in higher specific damping. The damping decreases at higher temperatures probably due to microstructural changes originating from Ni sintering.

Mechanical degradation due to redox cycling was observed during an experiment series carried out at isothermal temperatures of 750–790 °C. A decrease in Young's modulus was observed on cyclic re-oxidations and the loss of stiffness could be more or less linearly correlated with Cumulative Redox Strain measured from sample length change. Mechanical degradation due to damage started at about 0.5% dL/L_o strain, whereas a macroscopic loss of integrity of the samples resulted when redox strain exceeded about 2.5%. A simple isotropic continuum damage model was fitted to the elastic modulus degradation vs. CRS data.

Acknowledgements

The authors wish to thank Mr. Bart Bollen of IMCE NV, Belgium, for technical support and discussions during measurement campaigns in Diepenbeek, Belgium and at Risø, as well as Henrik Lund Frandsen of Risø DTU for useful input all through the work.

M. Pihlatie was financially supported by the Marie Curie Intra-European Fellowship, contract number MEIF-CT-2005-023882, as part of the European Commission's 6th framework programme. Other authors were supported by Energinet.dk under the project PSO 2007-1-7124 SOFC R&D.

References

1. Minh, N., Ceramic Fuel Cells. *J. Am. Ceram. Soc.*, 1993(3), 563–588.
2. Sarantaridis, D. and Atkinson, A., Redox cycling of Ni-based solid oxide fuel cell anodes: a review. *Fuel Cells*, 2007, **07**(3), 246–258.
3. Klemensø, T., PhD thesis. Technical University of Denmark, 2005.
4. Laurencin, J., Delette, G., Lefebvre-Joud, F. and Dupeux, M., A numerical tool to estimate SOFC mechanical degradation: case of the planar cell configuration. *J. Eur. Ceram. Soc.*, 2008, **28**, 1857–1869.
5. Sarantaridis, D. and Atkinson, A., Mechanical modelling of redox cycling damage in solid oxide fuel cells. In *Proceedings of the 7th European SOFC Forum, Lucerne, Switzerland*, 2006, paper P0728.
6. Giraud, S. and Canel, J., Young's modulus of some SOFC materials as a function of temperature. *J. Eur. Ceram. Soc.*, 2008, **28**, 77–83.
7. Radovic, M. and Lara-Curzio, E., Mechanical properties of tape cast nickel-based anode materials for solid oxide fuel cells before and after reduction in hydrogen. *Acta Mater.*, 2004, **52**, 5747–5756.
8. Radovic, M. and Lara-Curzio, E., Elastic properties of nickel-based anodes for solid oxide fuel cells as a function of the fraction of reduced NiO. *J. Am. Ceram. Soc.*, 2004, **87**(12), 2242–2246.
9. Morales-Rodríguez, A., Bravo-León, A., Domínguez-Rodríguez, A., Lopez-Esteban, S., Moya, J. S. and Jiménez-Melendo, M., High-temperature mechanical properties of zirconia/nickel composites. *J. Eur. Ceram. Soc.*, 2003, **23**, 2849–2856.
10. Morales-Rodríguez, A., Bravo-León, A., Richter, G., Rühle, M., Domíinguez-Rodrıíguez, A. and Jiménez-Melendo, M., Influence of oxidation on the high-temperature mechanical properties of zirconia/nickel cermets. *Scripta Mater.*, 2006, **54**, 2087–2090.
11. Selcuk, A. and Atkinson, A., Elastic properties of ceramic oxides used in solid oxide fuel cells (SOFC). *J. Eur. Ceram. Soc.*, 1997, **17**, 1523–1532.
12. Atkinson, A. and Selcuk, A., Mechanical behaviour of ceramic oxygen ion-conducting membranes. *Solid State Ionics*, 2000, **134**, 59–66.
13. Radovic, M., Lara-Curzio, E. and Riester, L., Comparison of different experimental techniques for determination of elastic properties of solids. *Mater. Sci. Eng.*, 2004, **A368**, 56–70.
14. Roebben, G., Basu, B., Vleugels, J., Van Humbeeck, J. and Van der Biest, O., The innovative Impulse Excitation Technique for high-temperature mechanical spectroscopy. *J. Alloys Compd.*, 2000, **310**, 284–287.
15. Roebben, G., Basu, B., Vleugels, J. and Van der Biest, O., Transformation-induced damping behaviour of Y-TZP zirconia ceramics. *J. Eur. Ceram. Soc.*, 2003, **23**, 481–489.
16. Sarantaridis, D., Chater, R. J. and Atkinson, A., Changes in physical and mechanical properties of SOFC Ni-YSZ composites caused by redox cycling. *J. Electrochem. Soc.*, 2008, **155**(5), B467–B472.
17. Pihlatie, M., Kaiser, A., Larsen, P. H. and Mogensen, M., Dimensional behaviour of Ni-YSZ anode supports for SOFC under RedOx cycling conditions. *ECS Trans.*, 2007, **7**(1), 1501–1510.
18. Roebben, G., Bollen, B., Brebels, A., Van Humbeeck, J. and Van der Biest, O., Impulse excitation apparatus to measure resonant frequencies, elastic moduli, and internal friction at room and high temperature. *Rev. Sci. Instrum.*, 1997, **68**(December (12)).
19. ASTM Standard E, 1876–99.
20. Nowick, A. S. and Berry, B. S., In *Anelastic Relaxation in Crystalline Solids*. Academic Press, New York, 1972.
21. Lakes, R. S., *Viscoelastic Solids*. CRC Press, 1998.
22. Liu, C., Huntz, A.-M. and Lebrun, J.-L., Origin and development of residual stresses in the Ni-NiO system: in-situ studies at high temperature by X-ray diffraction. *Mater. Sci. Eng. A*, 1993, **160**, 113–126.
23. du Plessis, P. de V., van Tonder, S. J. and Alberts, L., Elastic constants of a NiO single crystal: I. *J. Phys. C: Solid State Phys.*, 1971, **4**, 1983–1987.
24. Mori, M., Yamamoto, T., Itoh, H., Inaba, H. and Tagawa, H., Thermal expansion of nickel-zirconia anodes in solid oxide fuel cells during fabrication and operation. *J. Electrochem. Soc.*, 1998 April, **145**(4).
25. Simwonis, D., Tietz, F. and Stöver, D., Nickel coarsening in annealed Ni/8YSZ anode substrates for solid oxide fuel cells. *Solid State Ionics*, 2000, **132**, 241–251.
26. Sehested, J., Sintering of nickel steam-reforming catalysts. *J. Catal.*, 2003, **217**, 417–426.
27. Thydén, K., Liu, Y. L. and Bilde-Sørensen, J. B., Microstructural characterization of SOFC Ni-YSZ anode composites by low-voltage scanning electron microscopy. *Solid State Ionics*, 2008, **178**, 1984–1989.
28. Klemensø, T. and Mogensen, M., Ni-YSZ solid oxide fuel cell anode behavior upon redox cycling based on electrical characterization. *J. Am. Ceram. Soc.*, 2007, **90**(11), 3582–3588.